

Temperature, Cloud Structure, and Dynamics of Venus Middle Atmosphere by Infrared Remote Sensing from Pioneer Orbiter

Abstract. Further results from the Venus orbiter radiometric temperature experiment (VORTEX) on the Pioneer orbiter are presented. These are used to characterize the three-dimensional temperature field, the cloud structure, and the dynamics of the 60- to 130-kilometer altitude region of the Venus atmosphere. One of the new discoveries is a "dipole" structure at high latitudes, with two hot spots rotating around the pole, surrounded by banks of cold cloud.

As described in our earlier report (1), the Venus orbiter radiometric temperature experiment (VORTEX) is a multi-channel infrared radiometer similar to instruments flown on terrestrial weather satellites.

Temperature and cloud opacity profiles have been recovered from spectral radiance measurements by using zenith scanning and limb radiance inversion techniques. The former employs

multispectral observations of the same point on the planet at two or more emission angles (2); the latter involves viewing the atmosphere tangentially at the limb (3). Both are powerful methods for recovering separate temperature and cloud opacity profiles from radiance data. Only a small fraction of the 800,000 temperature profiles that were measured have been processed, but some general characteristics are apparent.

The mean lapse rate in the 65- to 85-km region is about 3.5 K/km, which compares well with a mean value of 3.9 K/km found by Venera 9 and Venera 10 experimenters using the radio occultation method (4). Between 95 and 105 km the atmosphere is nearly isothermal. Above 105 km the nighttime temperature decreases to a brightness temperature (assuming unit emissivity) as low as 120 K. Caution is needed in interpreting brightness temperatures above about 110 km as kinetic temperatures, since departures from local thermodynamic equilibrium may become important. However, consistency with the low nighttime exospheric (140 to 160 km) temperatures inferred from orbiter drag measurements (5) is implied. The limb radiance profiles obtained near periaapsis include evidence for an inflection in the lapse rate at about 72 km, and for tenuous cloud opacity ex-

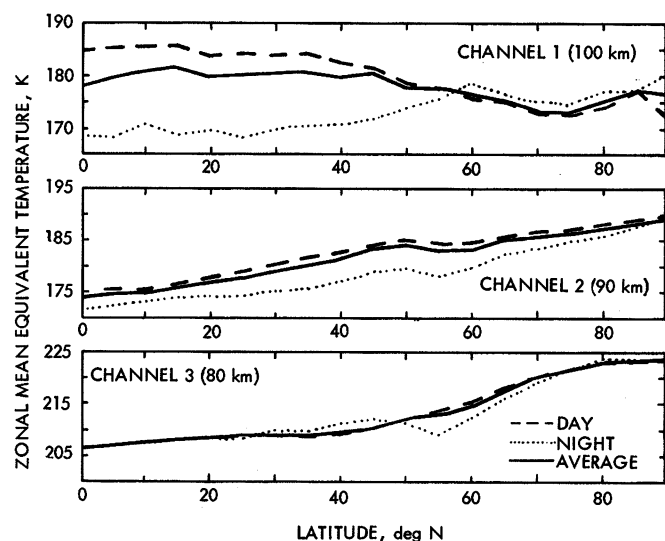
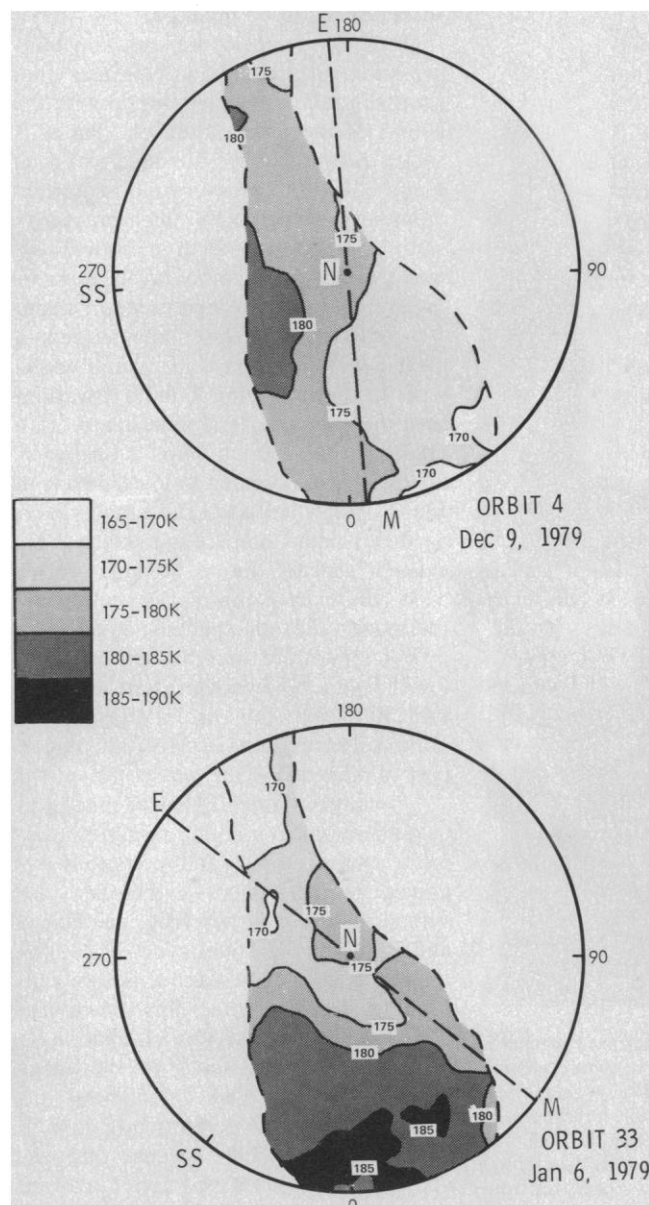


Fig. 1 (left). Contour maps of equivalent temperature (kelvins) derived from averaged calibrated pressure modulator radiometer measurements, sensitive to the altitude range 90 to 110 km. A polar stereographic projection in planet-centered celestial coordinates is used. Dashed lines represent the limits of coverage. Abbreviations: N, north pole; SS, subsolar celestial longitude; M, morning terminator; and E, evening terminator. Fig. 2. (right). Orbit 33 (5 January 1979) zonal mean equivalent temperature for three channels. Dayside, nightside, and full zonal means are shown; 73 percent of the measurements are on the dayside.

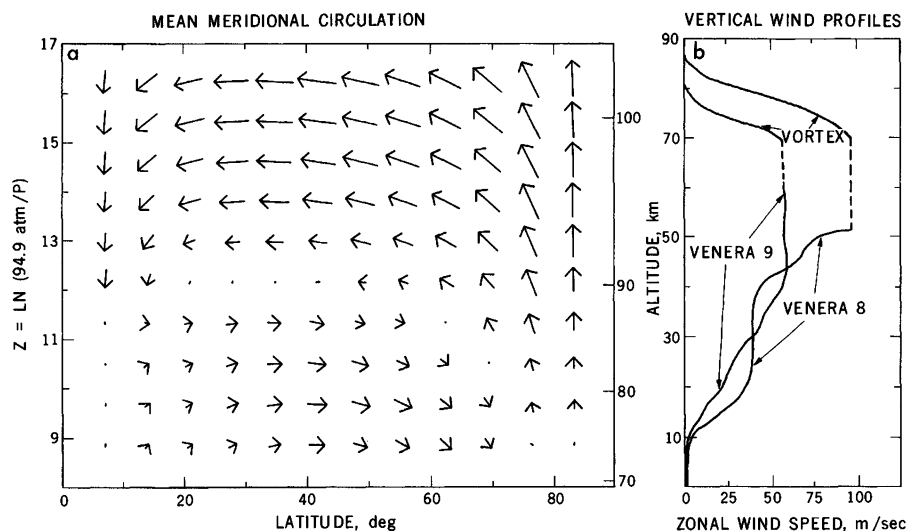


Fig. 3. (a) Wind vectors, calculated from a model in which the temperature field data are used as input, projected onto an altitude-latitude plane. The vertical scale is exaggerated relative to the horizontal: the largest vertical arrow corresponds to 30 cm/sec and the largest horizontal arrow to 60 m/sec. (b) Vertical profiles of the mean zonal wind derived from VORTEX data, assuming that the Venera 8 and Venera 9 measurements provide boundary values below 70 km. Dashed lines are extrapolations of the Venera profiles through the region where no data exist.

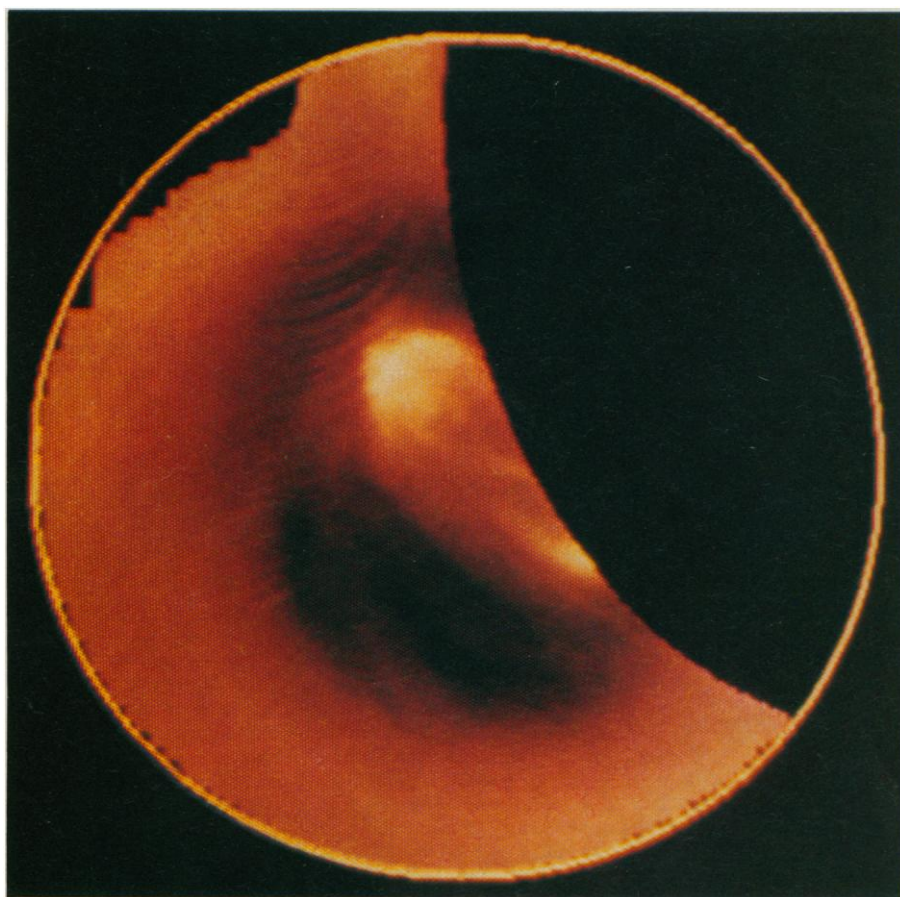


Fig. 4. High-resolution polar stereographic view of Venus generated from infrared measurements by VORTEX during orbit 69 on 11 February 1979. The north pole is at the center, and the enclosing circle represents 45°N latitude. The subsolar point is at the bottom. The wavelength of the measurements is in the 11.5- μ m atmospheric "window," so brighter regions correspond to warmer effective cloud top temperatures. Two bright features ("eyes") straddling the pole may be seen; these are connected by a warm S-shaped filament. The dark, cold cloud is the circum-polar collar described in the text. The dark streaks above the upper eye are artifacts arising from the scan pattern.

tending up to approximately 80 km. The latter is consistent with a nadir optical depth of 11.5 μ m of unity at about 68 km, plus a scale height of about 2 km, as inferred from zenith scanning observations over the same region of the planet. The limb radiance measurements in the 35- to 55- μ m channels are consistent with these cloud parameters, with no significant additional absorber. However, much greater 45- μ m darkening on the dayside suggests that there are important diurnal variations in the far infrared opacity in and above the main clouds. This could be due to small amounts of water vapor [see (6)]. Nadir viewing maps also show that the far infrared opacity is anomalously high over the pole, where the atmospheric temperatures are higher. Further studies are needed to establish whether the opacities observed are consistent with reasonable humidity levels, or whether an additional far infrared absorber needs to be invoked.

Maps of temperature on constant-pressure surfaces show contrasts that generally increase in amplitude with the height of the level observed. Figure 1 shows two such maps obtained on orbits 4 and 33 by the pressure modulator radiometer channel in its "high-pressure" setting. In this mode it measures the mean temperature of a layer approximately 20 km thick centered on about 100 km altitude. The maps suggest a clear dependence on solar zenith angle, with the dayside being 15 to 20 K warmer than the nightside. The diurnal structure present in the 100-km maps is further illustrated and extended to lower levels in Fig. 2. At low latitudes, the zonally averaged day-night temperature contrast increases sharply above 90 km. Above 60°N, the diurnal contrast is small. Furthermore, the unexpected equator-to-pole temperature increase observed at lower levels (1) is not present near 100 km. Maps for other orbits show small-scale daily variations of 5 to 10 K, due in part to planetary-scale waves (5).

A nonlinear model (7) has been used to calculate a mean circulation pattern, using measured zonally and temporally averaged temperatures. Values are assumed for the eddy viscosity coefficient and the cloud top zonal wind. These parameters have been varied, within reasonable limits, to test for sensitivity, with the result that the circulation is qualitatively independent of the exact values adopted. The calculations indicate that the positive equator-to-pole temperature gradient, present throughout most of the observed region, causes the mean zonal wind to decrease sharply

from its cloud top value of 100 m/sec (the so-called 4-day rotation), which reflects a balanced cyclostrophic flow, to nearly zero by about 80 km. This decrease (Fig. 3) is balanced by an increase in the advection and viscosity terms in the meridional momentum equation, and it reflects the diminishing role of cyclostrophic forces. This causes the mean meridional component of the wind to become large (60 m/sec) above 80 km, as shown in Fig. 3a.

Infrared imaging of the planet (Fig. 4) has revealed a great deal of fascinating structure, especially at the cloud top and in the polar region. Dark bands of high, cold cloud containing spiral filaments form a "collar" around the pole centered on approximately 65°N. The thickness of this feature varies with longitude and its detailed structure with time; its widest part is some 2000 km across, and this maximum appears to be phase-locked to the sun. The polar collar clouds in general are optically thick in the infrared and extend up to altitudes of 75 km. Inversion of multiple zenith measurements shows that this increase in effective cloud height is due either to an increase in the scale height of the cloud, from around 2 km, which is typical of most of the planet, to around 6 or 7 km in the polar collar, or to a second discrete layer overlying the main deck. The cloud opacity shows a marked wavelength dependence in the region 11 to 15 μm : everywhere outside the collar region the 11.5- μm brightness temperature is higher than that observed at 13 μm , but in the collar cloud this situation reverses. Numerical simulations in which multiple scattering algorithms are used to solve for the radiated intensity as a function of wavelength and angle show that the refractive index of an aqueous solution of 75 percent H_2SO_4 is sufficiently different at 11.5 and 13 μm to account for this observation. In particular, a model cloud with droplets 1 to 2 μm in radius is capable of fitting the data for certain distributions of number density with altitude.

Within the collar clouds, two bright features are located to either side of the pole. Fourier analysis of maps from successive orbits shows that the motion of this "dipole" can be interpreted, on average, as a retrograde motion about the pole with a 2.7-day period. This period matches well the observed average period of rotation of small-scale ultraviolet features seen at high latitudes in Mariner 10 images (8). However, both the rotation period of the dipole and the position of its axis relative to the pole appear to be variable from day to day. The 11.5-

μm temperatures within the bright "eyes" approach 260 K, the highest observed anywhere on the planet in this wavelength region, suggesting that they correspond to a lowering or clearing of the main cloud deck (9). Temperatures are higher in the atmosphere overlying the hot regions up to altitudes of at least 80 km, probably due to heating by thermal radiation from below. The two eyes are joined, in some of the images, by a bright S-shaped filament that passes near the center of rotation. Other bright filaments are sometimes seen extending across the cold collar cloud from one or the other eye. No ready explanation offers itself for these phenomena, but it is apparent that a simple vortex structure is no longer sufficient to explain the cloud structure at the pole. At the very least, such a circulation must be modified by a wavenumber 2 phenomenon surrounding the pole. We note in passing that wavenumber 2 disturbances are present in the terrestrial stratosphere in the form of Kelvin waves and tides (10), and that they play an important role in such phenomena as sudden warmings and the quasi-biennial oscillation. Furthermore, there is preliminary evidence for wavenumber 2 structure in equatorial and midlatitude regions on Venus from our temperature maps.

Finally, a preliminary analysis of data from the observations of reflected sunlight in the 0.4- to 5.0- μm albedo and 2.0- μm cloud height channels is strongly suggestive of the presence of a thin haze high above the main cloud deck. This haze covers the entire planet, including the polar collar and dipole features. The particle size is less than 0.5 μm , assuming spherical particles with refractive indices appropriate to a 75 percent H_2SO_4 solution. This haze presumably is the

same as that reported by Martonchik and Beer (11) from ground-based near-infrared spectroscopy.

F. W. TAYLOR

D. J. DINER, L. S. ELSON

D. J. MCCLEESE, J. V. MARTONCHIK
*Earth and Space Sciences Division,
Jet Propulsion Laboratory,
California Institute of Technology,
Pasadena 91103*

J. DELDERFIELD

S. P. BRADLEY, J. T. SCHOFIELD
*Atmospheric Physics Department,
University of Oxford, Oxford, England*

J. C. GILLE, M. T. COFFEY
*National Center for Atmospheric
Research, Boulder, Colorado 80302*

References and Notes

1. F. W. Taylor *et al.*, *Science* **203**, 779 (1979).
2. F. W. Taylor, *Appl. Opt.* **13**, 1559 (1974).
3. J. C. Gille and F. B. House, *J. Atmos. Sci.* **28**, 1427 (1971); J. C. Gille, P. L. Bailey, J. M. Russell, in preparation.
4. O. J. Yakovlev, A. I. Efimov, S. S. Matyugov, T. S. Timofeeva, E. V. Chub, G. D. Yakovleva, *Cosm. Res. (USSR)* **16**, 113 (1978).
5. G. M. Keating, F. W. Taylor, J. Y. Nicholson, E. W. Hinson, *Science* **205**, 62 (1979).
6. F. W. Taylor, *J. Atmos. Sci.* **32**, 1101 (1975).
7. L. S. Elson, *Geophys. Astrophys. Fluid. Dyn.* **10**, 319 (1978); in preparation.
8. S. Limaye and V. E. Suomi, *Bull. Am. Astron. Soc.* **9**, 509 (1977).
9. F. W. Taylor, D. J. McCleese, D. J. Diner, *Nature (London)*, in press.
10. J. R. Holton, *An Introduction to Dynamical Meteorology* (Academic Press, New York, 1972).
11. J. V. Martonchik and R. Beer, *J. Atmos. Sci.* **32**, 1151 (1975).
12. In addition to those acknowledged in our earlier report (1), we would like to thank the personnel in the JPL Photography Laboratory, especially D. Deats and R. Post, who have taken special pains on our behalf; the personnel of the NASA Communications Network at Jet Propulsion Laboratory, Goddard Spaceflight Center, Madrid, and London for supporting daily JPL-Oxford computer linkups; and R. Fimmel, J. Ferandin, and F. Schutz for their support. D.J.D. is a NASA-NRC Resident Research Associate. This report represents one phase of work carried out at the Jet Propulsion Laboratory, California Institute of Technology, under NASA contract NAS 7-100. The Oxford University contribution was funded by the U.K. Science Research Council.

15 May 1979

Further Results of the Pioneer Venus Nephelometer Experiment

Abstract. Backscattering data for the nephelometer experiments conducted aboard the Pioneer Venus mission probes, including data up to the highest altitudes measured by the probes, are presented. A few small signals were detected below the main cloud deck. Ambient radiation was measured at near-ultraviolet and visible wavelengths; the variation of extinction of near-ultraviolet with altitude is inferred. Ambient radiance decreased more rapidly at 530 than at 745 nanometers in the lower atmosphere.

In this report we present a more complete set of backscattering data than was available earlier (1, 2). In addition, we present data from the ultraviolet (UV) and visible channel radiometer experiments that were incorporated into the nephelometer instrument.

The results of the backscattering nephelometer measurements in the cloud regions are shown in Fig. 1. For comparison purposes, the data from each of the probes are plotted as a function of altitude above the sounder probe landing site (3). Although the protective window